Transistors based on ordered organic semiconductors

Schoonveld, Willem Alexander; Klapwijk, T.M

Chapter 2

Structure and growth of vacuum-evaporated organic thin films

The growth properties of high-vacuum evaporated thiophene-oligomer thin films on SiO_2 is explored both for (sub)-monolayer and for relatively large film thicknesses ($\sim$200 nm). The growth mode is characterized by a Volmer-Weber process. In the (sub)monolayer coverage regime, Oswald ripening phenomena dominate the island growth behaviour. The nucleation process shows a transition from initially formed 2D monolayer islands at low coverages to strongly facetted 3D islands at increasing coverages. The sizes of the individual crystallites are highly dependent on the substrate temperature. Large crystallites (up to $\sim$40 μm in diameter) are grown under conditions close to thermal equilibrium, i.e. with a very small supersaturation. We rationalize our results both from a kinetic and from a thermodynamic point of view. We show that optimum conditions for the growth of device-quality organic material are found close to the thermodynamic limit.

2.1 Introduction

Vacuum growth of thin films is usually performed under conditions far from thermal equilibrium, i.e., in supersaturation with the vapour phase. The crucial parameter in this context is the temperature of the substrate. In common deposition techniques such as MBE or CVD, the growth is performed at relatively low temperatures, and the vapour pressure of the growing film is negligible as compared to the deposit flux. Related to this, kinetic limitations such as diffusivities, and not thermodynamic factors such as surface- and interface free-energies, dominate the structure and morphology of the films. [1–4] Strikingly, both for metals and semiconductors, this does not preclude the preparation of high-quality films, with defect densities sufficiently low for electrical application.

One may however wonder whether this 'kinetic' growth regime is a general optimum in optimizing the quality of the grown films. The choice of the growth regime with respect to the solid-vapour phase-separation boundary determines whether kinetic or thermodynamic factors dominate the structure and morphology of the film.

In this work, we explore vacuum thin film growth in the latter extreme, approaching the thermodynamic limit. We report on the growth of crystalline organic thin films of quaterthiophene and extend this approach to other small rod-like molecules. We grow our films under quasi-equilibrium conditions, i.e., close to the solid-vapour (S-V) phase transition. The grown films are characterized using atomic force microscopy (AFM) and X-ray diffraction (XRD) experiments.

2.2 Experimental

In this chapter we focus on the structure and growth process of vacuum evaporated ordered organic thin films based on small rod like molecules like pentacene, quaterthiophene, α,α'-dihexylquaterthiophene and sexithiophene. In Section 2.2.3 we will characterize the thin films by means of XRD spectra as a function of the substrate temperature during the evaporation process, in order to explore the settings for which a highly ordered layered structure of the thin films is obtained. The next step is to optimize the sizes of the individual crystallites of the layered poly-crystalline thin film to at

least several microns in diameter, in order to be able to contact these crystals by means of standard photolithography and thus to fabricate single-crystal thin-film transistors. To this end we study the growth of these thin films with AFM in both the (sub)monolayer regime and at larger film thicknesses, as will be shown in section 2.2.4.

2.2.1 Overview of organic materials

The chemical structures of these molecules are shown in Fig. 2.1. The quaterthiophene (α-4T) and sexithiophene (α-6T) materials were commercially obtained from Syncom B.V. [5]. The α,α'-dihexylquaterthiophene (DH-4T) was obtained from Philips and also synthesized by Syncom. Both the sexithiophene and α,α'-dihexylquaterthiophene were additionally purified using a sublimation setup.

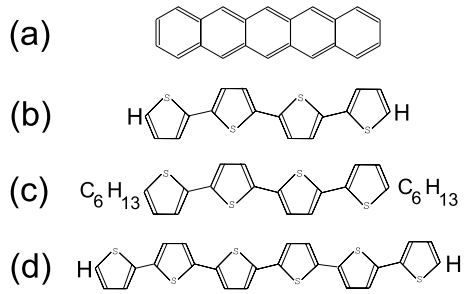

FIGURE 2.1. Chemical structure of **(a)** pentacene, **(b)** quaterthiophene, **(c)** α,α'-dihexylquaterthiophene and **(d)** sexithiophene.

2.2.2 High-vacuum evaporation setup

Highly doped Si-wafers, thermally oxidized in a dry atmosphere (SiO_2 thickness about 170 nm) are used as a substrate. The thin films are obtained by thermal evaporation (typical crucible temperatures are $\sim$180 °C for α-4T and $\sim$240 °C for pentacene) in a high-vacuum environment (see Fig. 2.2) with typical background pressures of 10^{-7} mbar. The material is loaded in a Ta crucible which is resistively heated. The temperature of the sample holder can be controlled in a large temperature range by resistive heating

elements and water cooling. The temperatures of the substrate and the crucible are monitored by chromel-alumel thermocouples. The deposition rate is monitored by an Intellemetrix IL 400 quartz oscillator. A shutter allows to adjust the evaporation rate to the desired value (within an accuracy of 0.1 nm/s) before the actual deposition of the thin film. After evaporation the substrate is rapidly cooled (rate ∼0.7 °C per second) to room temperature in order to prevent excessive desorption from the substrate.

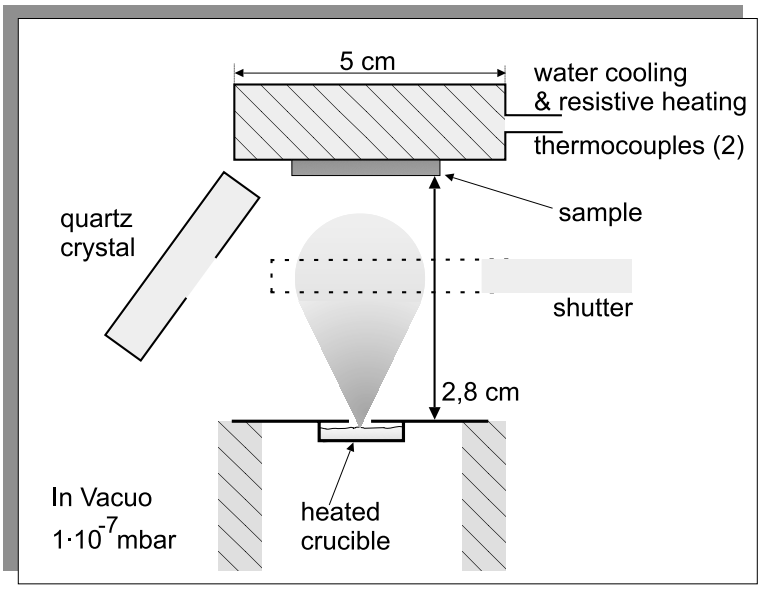

FIGURE 2.2. Experimental High-Vacuum evaporation setup.

2.2.3 Structure of ordered organic thin-films

Typically the structure of evaporated thin films of small rod-like molecules consists of a highly ordered layered structure in which the molecules stand nearly perpendicular to the substrate (see Fig. 2.3). [6–8] In Fig. 2.3(a) an AFM image is shown of an α-4T thin film of about 10 ML deposited on a mica substrate which clearly shows the steps and individual terraces of each molecular layer. The step height (1.88 nm) as deduced from the line scan shown in Fig. 2.3(b) is in good agreement with the vertical periodicity (15.4 Å) as

obtained from XRD experiments (see schematic view in Fig. 2.3(c)). Thus the height of each mono-molecular layer roughly corresponds to the length of one molecule. Similar results were obtained by Böhme et al. [9,10] who also showed mono-molecular steps for quinquethiophene thin films in the (sub)monolayer coverage regime. This kind of ordering is typically observed for a variety of (insulating) substrates like glass, SiO_2, quartz and PMMA but also on Indium-Tin-Oxide (ITO). However, from scanning tunneling microscopy experiments on (sub)monolayer coverages of end-capped quinquethiophene and quaterthiohene on Ag(111), an alternative structure was reported in which the molecules orient in a flat-lying fashion. [11,12]

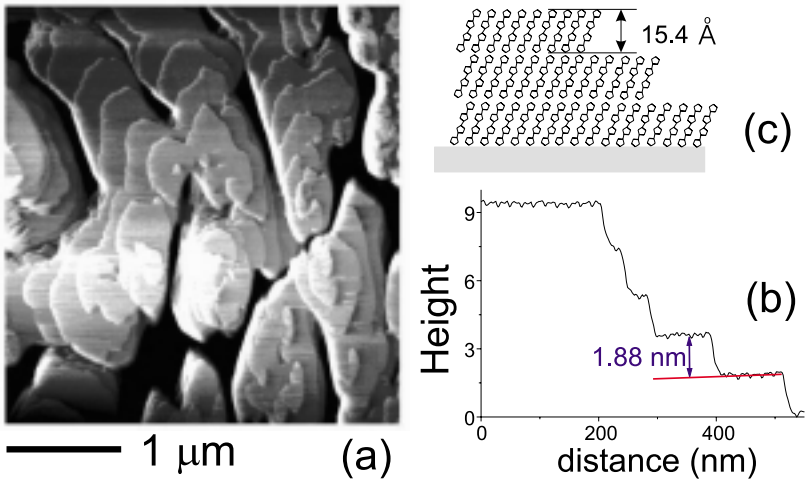

FIGURE 2.3. **(a)** AFM image of 10 monolayers of α-4T on mica, **(b)** linescan of an AFM image showing the individual mono-molecular steps and **(c)** schematic overview of three molecular layers.

The Θ-2Θ X-ray diffraction data of the thin films based on the materials shown in Fig. 2.1 are shown in Fig. 2.4. For all materials a spectrum with sharply resolved diffraction peaks is obtained, which indicates a layered structure of the thin films with a layer spacing given by the first diffraction peak (see Fig. 2.4).

All spectra were taken from thin films deposited with the substrate at room temperature, except for the sexithiophene thin film which was evaporated at 180 °C substrate temperature. The thin-film structure of sexithio-

phene is strongly dependent on the used substrate temperature and shows several polymorphs. [13] Only at a substrate temperature of 180 °C during evaporation we observed the sharply peaked XRD spectrum. [14] At this point it is not clear whether this is an intrinsic phenomenon of sexithiophene or an impurity induced effect. Also note the doubly peaked spectrum at every diffraction order for the pentacene thin-film. This indicates the co-existence of two phases in the thin film: a thin film phase (layer spacing 15.5 Å) and a pentacene bulk phase with layer spacing 14.5 Å. More details about the origin of these two phases is outlined in Chapter 3. The XRD spectra of both α-4T and α,α'-dihexylquaterthiophene show no dependence on the used substrate temperatures, which indicates that the layered structures of the thin films remain identical.

It should be noted that with XRD spectra of (evaporated) thin films one is only sensitive to a periodicity in a direction perpendicular to the substrate and thus XRD spectra only yield the mono-molecular layer spacing in case of a layered thin film structure. For a full characterization of the crystal unit-cell one needs to measure the XRD spectra in all possible crystal axis directions. In order to carry out these experiments one thus needs a macroscopic single crystal instead of thin films. We have listed the unit-cell parameters of the relevant materials in Table 2.1. These number are based on the available data in the literature obtained with macroscopic single crystals. In this table we listed both the high- and low-temperature single crystal polymorph data of α-4T and α-6T. However, in comparison to our experiments only the low-temperature data are in the relevant temperature regime.

TABLE 2.1. Crystallographic parameters based on single crystal data

parameter	material				
	α-4T (LT) [15]	α-4T (HT) [15,16]	α-6T (LT) [17]	α-6T (HT) [18]	pentacene [19,20]
space group	$P2_1/c$	$P2_1/a$	$P2_1/n$	$P2_1/a$	$P\bar{1}$
a (Å)	6.08	8.93	6.03	9.14	7.90
b (Å)	7.86	5.75	7.85	5.68	6.06
c (Å)	30.48	14.34	44.71	20.67	16.01
Z	4	2	4	2	2

Comparing the values of the layer spacing of the thiophene oligomers obtained from Fig. 2.4 to those of the low-temperature polymorph listed in Table 2.1, we observe that the layer spacing is equal to half the length of the c-direction of the unit-cell (The number of molecules in the unit cell Z is 4). After correction of the factor two we still observe a small difference in the layer spacing, which can be attributed to a slightly different crystal structure of the thin film geometry in comparison to the single crystal data. [8]

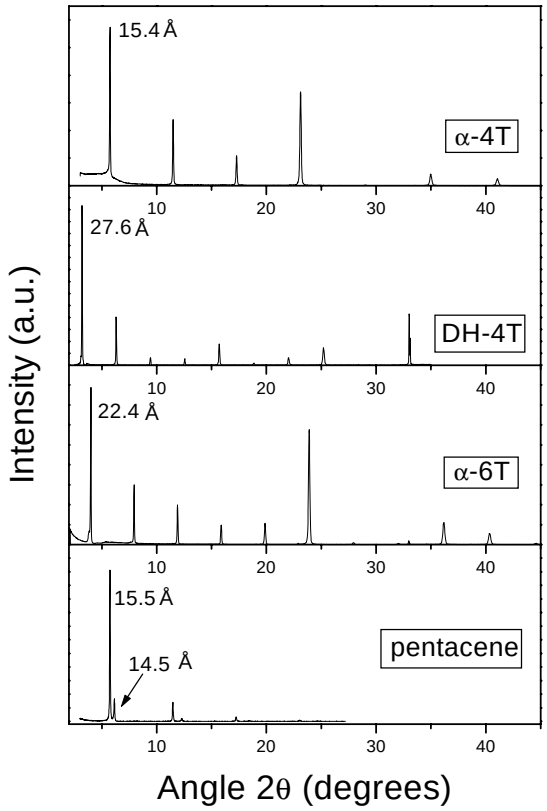

FIGURE 2.4. Θ-2Θ X-ray diffraction data of evaporated thin films of the used materials. The sharp diffraction peaks correspond to the vertical periodicity in the (00l) direction perpendicular to the substrate. The layer spacings are indicated at the first order diffraction peaks.

2.2.4 Growth and morphology of ordered organic thin-films

In order to reach high quality organic thin films for device applications it is strongly desirable to study the growth properties of organic molecules for the relevant substrates. In this section we focus on the growth properties of α-4T material onto SiO_2 substrates in order to obtain single crystal thin-film transistors. From (sub)monolayer coverage studies of quinquethiophene on SiO_2 [10] a Stranski-Krastanov type of growth has been inferred, in which first two completely covered monolayers are formed on the substrate whereafter a 3D growth mode sets in. However, other studies of 100 nm thin films of sexithiophene on mica revealed (sub)micron sized 3D grains and it was not clear whether or not completely covered monolayers were formed prior to the 3D grains. The sizes of these grains were shown to increase upon using increased substrate temperatures, indicating that the growth mode is a diffusion-limited process. [21,22]

Growth studies in the (sub)monolayer coverage regime

The morphology of α-4T thin films in the (sub)monolayer regime is studied with AFM as a function of the amount of material deposited using a constant evaporation rate (~ 0.3 Å/sec) and substrate temperature (295 K). [23] These experiments were performed under UHV conditions with an experimental setup similar to that shown in Fig. 2.2. The morphology of two different stages of the growth process is shown in Fig. 2.5. In the initial growth stage we find a large number of mono-layer islands which cover almost 50% of the substrate (see Fig. 2.5(b)). With increasing film thickness, the number of islands has decreased dramatically and each island (already micron sized!) shows a strong facetting behaviour with a uniform height of 24 nm (see Fig. 2.5(a)). The facetting directions correspond to the herringbone direction which is the most densely packed crystal axis direction within the unit-cell (see also Fig. 4.5). Apparently, the surface free energy along the herringbone direction is lower than for other unit cell directions which results the crystal growing prefereable along this direction and thus showing facetting behaviour.

The remarkable decrease of the island density with increased film coverage is ascribed to a process called Oswald ripening [2,3]. This process is characterized by the diffusion of material from small islands with high "vapour"

pressures to large islands with low "vapour" pressures. Consequently the initially larger islands will grow at the expense of the smaller ones. The "vapour" pressure of an island is given by the total free energy of the island, which is described by thermodynamic arguments like surface and interface free-energies. On islands with a large total free energy, the molecules will be bound weakly, which results in a higher "vapour" pressure around these islands. This process is clearly demonstrated by an AFM image (not shown) in the submonolayer coverage regime (similar to Fig. 2.5(b))), showing one large island surrounded by mono-molecular height islands outside a depletion zone of 7 microns. Material volume analysis indicated that the large island has grown at the expense of the mono-molecular islands within its depletion zone. This sustaines the suggestion that Oswald ripening is the driving force.

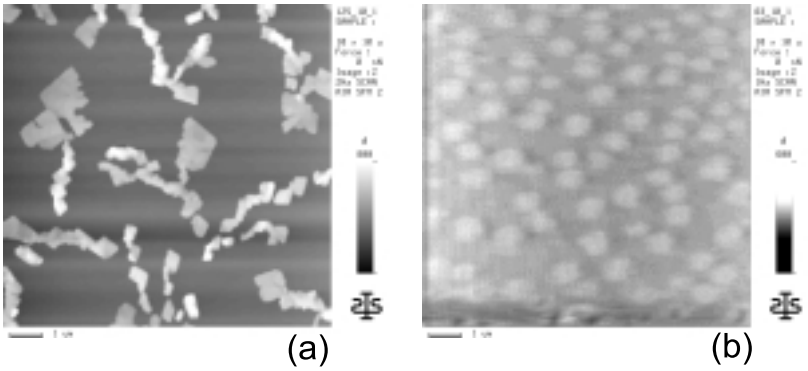

FIGURE 2.5. AFM images showing **(a)** strongly facetted islands with several monolayers of deposited material, and **(b)** monolayer islands in the (sub)monolayer coverage regime.

In Fig. 2.6 we analyzed a series of samples with increasing film thickness. The morphology of the thin films is divided in two sections. In the initial growth stage, at coverages below 1 monolayer, the islands are 2-dimensional (2D) and at coverages above 1 monolayer a transition is observed from 2D to 3D islands, similar to what was discussed above. The growth is characterized by a Volmer-Weber type of process. In contrast to the observation of Böhme et al. [9], we do not observe the formation of a completely covered monolayer before the 3D island growth sets in.

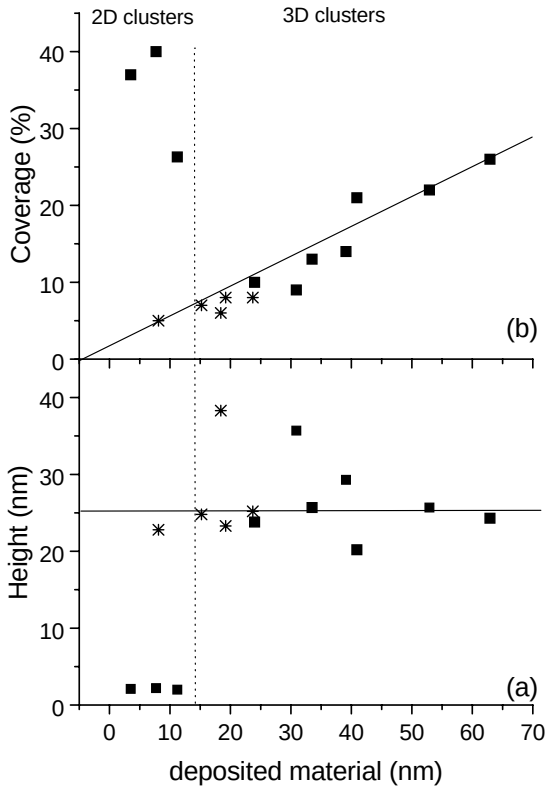

FIGURE 2.6. **(a)** The average height of the islands and **(b)** the coverage (in percentage of the substrate), as a function of the amount of deposited material. The data points marked with a asterisk (*) are obtained on additionally purified material.

In the initial growth stage, the substrate is covered for almost 50% with monolayer islands. After an initial drop in the substrate coverage percentage owing to the transition to 3D islands, a continuous increase of the substrate coverage with the deposited amount of material is observed (indicated by the straight solid line in Fig. 2.6(b)). The height of the 3D islands is observed to saturate at 24 nm (about 12 monolayers). Thus once the 3D islands have formed they can be characterized by a uniform height of 12 monolayers. Upon depositing more material, these islands tend to grow in lateral direc-

tions (the number of islands is a constant as a function of layer thickness). That the height of these islands is constant is a rather surprising observation. Apparently, the free energy of these islands, which is given by the interface and bulk free-energies, is for a height of 12 monolayers about equal to or less than the surface free energy of the substrate. Thus from this point forward, it is energetically more favourable for the island to grow in lateral direction along the substrate, in order to minimize the total free energy of the system.

The additionally purified material (see data points marked with a asterisk (*) in Fig. 2.6) does not show the formation of 2D monolayer islands at low film coverages. Instead, 3D islands are formed with extremely large inter-island separation (∼100 μm). Apparently the unintentional impurities in the α-4T material act as surfactant for the growth of the monolayer islands. The large inter-island spacing of the pure material at low coverages indicates that the typical diffusion length of the molecules on SiO_2 is already very large, even for substrates at room temperature!

Obtaining large single crystals within a poly-crystalline thin film

At room temperature the average size of the crystallites of an organic thin film is about 100 nm. [13,21,25] The sizes of these crystallites can be substantially improved to diameters of several microns by a Rapid Thermal Annealing process. [24,25] With this technique, the organic thin film is rapidly heated above its melting point at ambient conditions, after which it is slowly cooled down to facilitate recrystallization, resulting in crystals with increased sizes. Another technique, also commonly used when growing high quality thin films of inorganic materials, is evaporating the organic material onto a substrate which is at an elevated temperature.

In this section we report on the increased sizes of the crystallites within the thin film using an elevated substrate temperature during evaporation. At these higher substrate temperatures, the diffusion length of the molecules along the substrate is enhanced and allows for the formation of a limited number of nucleation sites in the initial stages of growth, whereafter a 3D growth of these islands sets in without formation of additional nucleation sites. Using this approach we are able to enhance the crystallite sizes of α-4T thin films from ∼100 nm at room temperature substrates to ∼40 μm at substrate temperatures of 80°C (see Fig. 2.7). The obtained crystallites are all strongly facetted which represent the equilibrium shape of these crystals.

As is shown in the evaporation "phase diagram" of Fig. 2.7, the thin film morphology using elevated substrate temperatures can be divided in three different types strongly depending on the combination of both the evaporation rate and the actual substrate temperature. At the elevated substrate temperatures, not only the diffusion of the molecules along the substrate but also the process of re-evaporation of the molecules from the substrate is significantly enhanced.

The latter process is roughly determined by the sublimation temperature of the organic material in relation to the used substrate temperature and sets a lower limit to the source evaporation rate necessary to have a net growth of the thin film. The figures representing the different morphologies labeled I, II and III are taken using an optical microscope with polarizing elements (see Chapter 4). The thin film of region I is characterized by very large crystallites with large inter-island separations. The crystallites are not homogeneously filled and show a dendrite-like structure. The structure of region I is typically observed for a low evaporation rate in comparison to the substrate temperature and, consequently, the re-evaporation rate. If the evaporation rate is lowered even further, there will be no net growth of the thin film at all. A morphology which is more desirable for fabrication of single-crystal thin film transistors is given by region II. In this region with a larger evaporation rate in comparison to region I, a large number of crystallites with diameters of about 20 μm are formed, which are homogeneously shaped and again show facetting behaviour. This region is typically referred to as the region with optimal settings of both the evaporation rate and substrate temperature (as indicated by the straight line in Fig. 2.7). For even larger evaporation rates, above the optimal settings, we observe that the crystal consists of a cluster of small fractions separated by large crevices and each fraction has an identical orientation. It is obvious that also this morphology is not desired for device applications since crevices are expected to conduct poorly.

This approach of optimizing the thin film morphology by exploring the evaporation phase diagram of Fig. 2.7 can be generalized to all materials listed in Fig. 2.1. We typically find that upon raising the substrate temperature, the crystallite size increases. To maximize the yield for fabricating single-crystal TFTs, one would like the entire substrate to be covered with large crystals. This means that the crystal density should be large and that

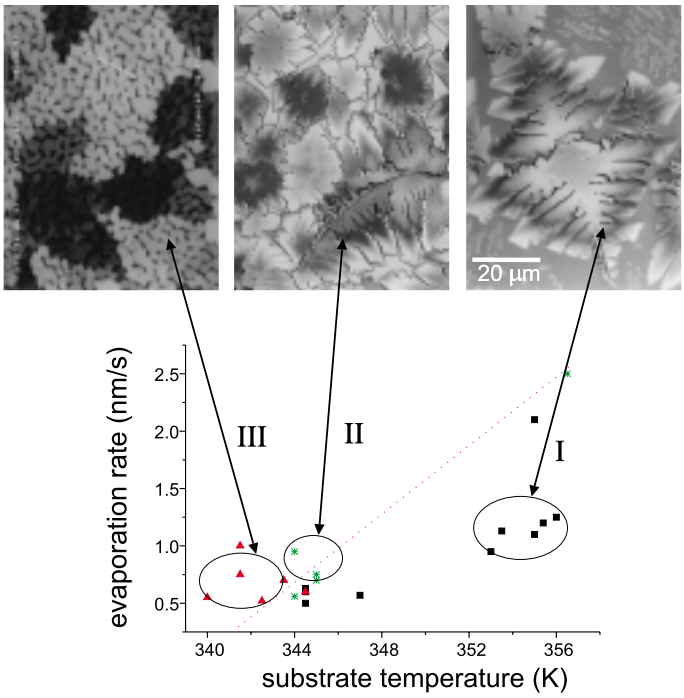

FIGURE 2.7. Three different types of α-4T thin-film morphology for several combinations of the substrate temperature and the evaporation rate from the source. The straight line is a guide to the eye and marks the optimal settings (morphology type II) in order to obtain large individual crystallites within a poly-crystalline thin film.

the crystals are preferably uniformly shaped (morphology type II). To this end the evaporation rate from the source should be slightly larger than the re-evaporation rate from the substrate. In this case, the latter is determined by the used substrate temperature in relation to the sublimation rate of the material.

2.2.5 Discussion and conclusions

We have demonstrated that evaporated thin films of small rod-like molecules result in highly ordered thin films with a layered structure in which the molecules stand nearly perpendicular to the substrate. The individual crystallite sizes can be drastically improved from ~100 nm to several tens of

microns depending on the evaporation parameters. The growth mode is described by a Volmer-Weber type of process in which the nucleated islands have a 3-dimensional growth mode without the formation of an initial complete monolayer.

Based on the here presented experiments of α-4T-on-SiO_2 we conjecture that the growth mode is described in the thermodynamic regime in which surface- and interface free-energies dominate the structure and morphology of the films. In the kinetic growth mode regime, which is commonly used for epitaxial growth of inorganic materials, the formed nuclei are already stable for clusters of two or more atoms and are in strong supersaturation with the vapour phase. In this regime, the vapour pressure of the thin films is negligible compared to the depositing flux. In thin films with (sub)monolayer coverages we have shown that Oswald ripening is an important process determining the thin film growth. In this process the total free energy of the thin film is minimized in terms of thermodynamic arguments, large islands with low total free energy grow at the expense of less stable smaller islands. Next to this effect, large strongly facetted crystallites are obtained using increased substrate temperatures together with an evaporation rate just above the re-evaporation rate from the substrate, which means that the molecules of the islands are in dynamic equilibrium with the vapour phase of the source, unlike the case of the supersaturation regime in the kinetic growth process. These aspects of growth of ordered organic thin films indicate that these films are grown in the thermodynamic limit in which Oswald ripening and small supersaturations are important aspects of growth.

References

[1] J.A. Venables, G.D.T. Spiller and M. Hanbücken, Rep. Prog. Phys. **47**, 399 (1984).

[2] K.N. Tu, J.W. Wagner and L.C. Feldman, *Electronic thin film science for electrical engineers and materials scientists*, Macmillan Publishing compagny (1992).

[3] I.V. Markov, *Crystal growth for beginners*, World Scientific (1995).

[4] C. Günther, S. Günther, E. Kopatzki, R.Q. Hwang, J. Schröder, J. Vrijmoeth and R.J. Behm, Ber. Bunsenges. Phys. Chem. **97**, 522 (1993).

[5] Syncom B.V., Nijenborgh 4, 9747 AG Groningen, The Netherlands.

[6] F. van Bolhuis, H. Wynberg, E.E. Havinga, E.W. Meijer and E.G.J. Staring, Synth. Metals **30**, 381 (1989).
[7] W.Porzio, S. Destri, M. Mascherpa and S. Brückner, Acta. Polymer. **44**, 266 (1993).
[8] S. Hotta and K. Waragai, Adv. Mater. **5(12)**, 896 (1993).
[9] O. Böhme, Ch. Ziegler and W. Göpel, Adv. Mater. **6(7/8)**, 587 (1994).
[10] O. Böhme, Ch. Ziegler and W. Göpel, Synth. Metals **67**, 87 (1994).
[11] A. Soukopp, K. Clöckler. P. Bäuerle, M. Sokolowski and E. Umbach, Adv. Mater. **8**, 906 (1996).
[12] W. Gebauer, M. Bässler, A. Soukopp, C. Väterlein, R. Fink, M. Sokolowski and E. Umbach, Synth. Metals **83**, 227 (1996).
[13] B. Servet, G. Horowitz, S. Ries, O. Lagorsse, P. Alnot, A. Yassar, F. Deloffre, P. Srivastava, R. Hajlaoui, P. Lang, and F. Garnier, Chem. Mat. **6**, 1809 (1994).
[14] D.B.A. Rep, M. Sc. thesis (University of Groningen) 1997.
[15] T. Siegrist, C. Kloc, R.A. Laudise, H.E. Katz and R.C. Haddon, Adv. Mater. **10(5)**, 379 (1998).
[16] L. Antolini, G. Horowitz, F. Kouki and F. Garnier, Adv. Mater. **10(5)**, 382 (1998).
[17] G. Horowitz, B. Bachet, A. Yassar, P. Lang, F. Demanze, J.L. Fave and F. Garnier, Chem. Mater **7**, 1337 (1995).
[18] T. Siegrist, R.M. Fleming, R.C. Haddon, R.A. Laudise, A.J. Lovinger, H.E. Katz, P. Bridenbaugh and D.D. Davis, J. Mater. Res. **10(9)**, 2170 (1995).
[19] E.A. Silinsh and V. Càpek, *Organic Molecular Crystals*, AIP press, New York (1994).
[20] R.B. Campbell, J. M. Robertson, Acta Cryst. **15**, 289 (1962).
[21] F. Biscarini, R. Zamboni, P. Samori, P. Ostoja and C. Taliani, Phys. Rev. B **52**, 14868 (1995).
[22] F. Biscarini, P. Samori, O. Greco and R. Zamboni, Phys. Rev. Lett. **78**, 2389 (1997).
[23] R. Veldman, M. Sc. thesis (University of Groningen) 1996.
[24] A.J. Lovinger, D.D. Davis, A. Dodabalapur, H.E. Katz and L. Torsi, Macromolecules **29**, 4952 (1996).
[25] L. Torsi, A. Dodabalapur, A.J. Lovinger, H.E. Katz, R. Ruel, D.D. Davis and K.W. Baldwin, Chem. Mater. **7**, 2247 (1995).